



# Estimation of the depth limit for percussion drilling with picosecond laser pulses

DANIEL J. FÖRSTER,<sup>1,2,\*</sup> RUDOLF WEBER,<sup>1</sup> DANIEL HOLDER,<sup>1</sup> AND THOMAS GRAF<sup>1</sup>

<sup>1</sup>Institut für Strahlwerkzeuge IFSW, Pfaffenwaldring 43, 70569 Stuttgart, Germany

<sup>2</sup>Graduate School of advanced Manufacturing Engineering GSaME, Nobelstrasse 12, 70569 Stuttgart, Germany

\*[daniel.foerster@ifsw.uni-stuttgart.de](mailto:daniel.foerster@ifsw.uni-stuttgart.de)

**Abstract:** We present a model to predict the final depth of percussion-drilled holes that are produced with picosecond laser pulses in metals. It is based on the assumption that boreholes always have conical geometries when the drilling process terminates. We show that the model is valid for various process parameters when drilling in stainless steel. This was even confirmed by drilling with 3 mJ pulses which resulted in a 10 mm deep borehole without thermal damage.

© 2018 Optical Society of America under the terms of the [OSA Open Access Publishing Agreement](#)

**OCIS codes:** (140.3390) Laser materials processing; (350.3850) Materials processing.

## References and links

1. M. Kraus, M. A. Ahmed, A. Michalowski, A. Voss, R. Weber, and T. Graf, "Microdrilling in Steel using Ultrashort Pulsed Laser Beams with Radial and Azimuthal Polarization," *Opt. Express* **18**(21), 22305–22313 (2010).
2. A. Weck, T. Crawford, D. Wilkinson, H. K. Haugen, and J. S. Preston, "Laser drilling of high aspect ratio holes in copper with femtosecond, picosecond and nanosecond pulses," *Appl. Phys., A Mater. Sci. Process.* **90**(3), 537–543 (2008).
3. M. Kraus, D. Walter, A. Michalowski, and J. König, "Processing Techniques and System Technology for Precise and Productive Microdrilling in Metals," *Ultrashort Pulse Laser Technology* (Springer International Publishing, 2016), pp. 201–230.
4. G. Umlauf, E. Zahedi, C. Wörz, J. Barz, M. Liewald, T. Graf, G. Tovar "Grundlagenuntersuchungen zur Herstellung von Lasermikrobohrungen in Stahl und dem Ausströmverhalten von CO<sub>2</sub> als Trockenschmiermedium," *Dry Met. Forming OAJ FMT 2* 018–049 (2016).
5. D. J. Förster, R. Weber, and T. Graf, "Residual heat during ultrashort laser drilling of metals," *Proceedings of LPM2017 - the 18th International Symposium on Laser Precision Microfabrication* (2017)
6. D. Breiting, A. Ruf, and F. Dausinger, "Fundamental aspects in machining of metals with short and ultrashort laser pulses," *Proc. SPIE* **5339**, 49–64 (2004).
7. S. Döring, S. Richter, S. Nolte, and A. Tünnermann, "In situ imaging of hole shape evolution in ultrashort pulse laser drilling," *Opt. Express* **18**(19), 20395–20400 (2010).
8. S. Döring, "Analysis of the hole shape evolution in ultrashort pulse laser drilling," (Cuvillier Verlag, 2014).
9. A. Michalowski, "Untersuchungen zur Mikrobearbeitung von Stahl mit ultrakurzen Laserpulsen," (Herbert Utz Verlag, 2014)
10. G. Raciukaitis, M. Brikas, P. Gecys, and M. Gedvilas, "Accumulation effects in laser ablation of metals with high-repetition-rate lasers," *Proc. SPIE* **7005**, 70052L (2008).
11. A. Ancona, F. Röser, K. Rademaker, J. Limpert, S. Nolte, and A. Tünnermann, "High speed laser drilling of metals using a high repetition rate, high average power ultrafast fiber CPA system," *Opt. Express* **16**(12), 8958–8968 (2008).
12. R. Weber, T. Graf, P. Berger, V. Onuseit, M. Wiedenmann, C. Freitag, and A. Feuer, "Heat accumulation during pulsed laser materials processing," *Opt. Express* **22**(9), 11312–11324 (2014).
13. F. Di Niso, C. Gaudioso, T. Sibillano, F. P. Mezzapesa, A. Ancona, and P. M. Lugarà, "Role of heat accumulation on the incubation effect in multi-shot laser ablation of stainless steel at high repetition rates," *Opt. Express* **22**(10), 12200–12210 (2014).
14. Y. Qin, A. Michalowski, R. Weber, S. Yang, T. Graf, and X. Ni, "Comparison between ray-tracing and physical optics for the computation of light absorption in capillaries-the influence of diffraction and interference," *Opt. Express* **20**(24), 26606–26617 (2012).
15. A. Gouffé, "Correction d'ouverture des corps-noirs artificiels compte tenu eds diffusions multiples internes," *Revue d'Optique* **24**, 1–10 (1945).
16. A. Gouffé, "Aperture Corrections of Artificial Black Bodies with Consideration of Multiple Internal Diffusions," *General dynamics/Astronautics, San Diego, CA* (1960)

17. C. Banas, "High power laser welding," *The Industrial Laser Annual Handbook*, **102** (104) (Pennwell Books Tulsa, 1986), p. 69.
18. F. Fetzter, P. Stritt, P. Berger, R. Weber, and T. Graf, "Fast numerical method to predict the depth of laser welding," *J. Laser Appl.* **29**(2), 022012 (2017).
19. H. Hügel and T. Graf, *Laser in der Fertigung*, 3rd ed. (Springer Vieweg, 2014)
20. B. Neuenschwander, B. Jaeggi, M. Schmid, A. Dommann, A. Neels, T. Bandi, and G. Hennig, "Factors controlling the incubation in the application of ps laser pulses on copper and iron surfaces," *Proc. SPIE* **8607**, 86070D (2013).
21. J.-P. Negel, A. Voss, M. A. Ahmed, D. Bauer, D. Sutter, A. Killi, and T. Graf, "1.1 kW average output power from a thin-disk multipass amplifier for ultrashort laser pulses," *Opt. Lett.* **38**(24), 5442–5445 (2013).
22. B. Jaeggi, B. Neuenschwander, M. Schmid, M. Murali, J. Zuercher, and U. Hunziker, "Influence of the pulse duration in the ps-regime on the ablation efficiency of metals," *Phys. Procedia* **12**, 164–171 (2011).
23. H. Pantisar, P. Laakso, and R. Penttilä, "Material removal rates of metals using UV and IR picosecond pulses," *Proceedings of the 4th International WLT-conference on Lasers in Manufacturing* (2007).
24. S. M. Klimentov, T. V. Kononenko, P. A. Pivovarov, S. V. Garnov, V. I. Konov, A. M. Prokhorov, D. Breitling, and F. Dausinger, "The role of plasma in ablation of materials by ultrashort laser pulses," *Quantum Electron.* **31**(5), 378–382 (2001).
25. S. M. Klimentov, S. V. Garnov, V. I. Konov, T. V. Kononenko, P. A. Pivovarov, O. G. Tsarkova, D. Breitling, and F. Dausinger, "Effect of low-threshold air breakdown on material ablation by short laser pulses," *Phys. Wave Phenom.* **15**(1), 1–11 (2007).
26. A. Feuer, M. Kraus, V. Onuseit, R. Weber, T. Graf, D. Ingildeev, and F. Hermanutz, "Laser Drilling of High-Quality Microhole Arrays for Super-Micro Fibre Production," *7th International Conference & Exhibition on Photonic Technologies* (2012)

## 1. Introduction

Drilling of metals, ceramics, and semiconductors with ultrashort laser pulses is an established and widely used process. If the quality of the boreholes needs to be very high, often advanced strategies such as helical drilling are used [1–4]. The deviations from the desired drilling geometry are within the order of one micrometer and thermal damage can be completely avoided. Percussion drilling as a basic drilling process is ideally suited to perform fundamental experiments. Today, hole depths of a few millimeters with aspect ratios of up to 20 can be achieved [5]. Regardless of the drilling strategy used, from a certain number of applied pulses there is first a slowdown in the drilling progress, which finally results in a termination of the process. This fundamental behavior is mainly due to the lowering of the available energy at the tip of the borehole. An end of the drilling process takes place when the fluence falls below the ablation threshold [5–9]. Depending on the process parameters such as the pulse energy, the repetition rate, the pulse duration, the wavelength and the focusing conditions as well as the used materials, the quality of a borehole obtained after a percussion drilling process ranges from holes with steep inner walls and smooth surfaces to highly irregular shapes. The occurrence of such irregularities and thus mostly unwanted geometries can be attributed to specific absorption mechanisms (i.e. multi-photon absorption in the case of semiconductors) [7,8] and, especially in the case of metals, to heat accumulation effects associated with an excessive generation of melt [5, 10–13]. The heat accumulation associated with increasing repetition rate in practice is particularly noticed at repetition rates of 100 kHz and higher [5,10–13]. While on the one hand these effects can significantly reduce the quality of laser-drilled holes, the drilling efficiency can be improved with regard to shorter drilling times [5,11,13], since the material removal by evaporation or sublimation is substituted mainly by the less energy consuming melt expulsion. Generally, the increasing influence of melt needs to be prevented, e.g. by drilling with ultra-short pulses close to the ablation threshold and at moderate repetition rates to ensure a good processing quality. During percussion drilling with ultra-short laser pulses, conical geometries are formed [6–9], as long as the discussed effects leading to irregularities such as multi-photon absorption [7,8] and heat accumulation [5,10–13] are avoided. Based on this fact, an idealized analytical model is introduced in the following which allows to estimate the achievable hole depth or aspect ratio, respectively, with regard to only one process parameter, i.e. the fluence (cf. section 2). Furthermore, the experimental validation of this model is shown in section 3. Being of high interest for different applications, the material of choice was stainless steel (St 1.4301 or AISI 304). In section

4 it is finally shown how the model was used to design a deep-drilling process which allowed to reproducibly produce 10 mm deep holes using a high-energy ultra-short pulsed laser.

## 2. Termination of a percussion drilling process

High-quality percussion-drilled holes avoiding thermal damage and excessive melting commonly are of a conical shape and are subject to limitations with respect to depth and aspect ratio. The goal of this section is to derive a simplified model in order to be able to predict these limitations and to design the drilling process to attain a specified depth or aspect ratio. The model is based on the simplified assumption that the formation of a laser-drilled hole naturally stops as soon as the incident local fluence  $\Phi$  drops below the ablation threshold  $\Phi_{th}$  everywhere on the walls of the hole. Note that this assumption does not apply if the hole geometry is further modified by a flow of molten material which may occur also below the actual ablation threshold. Hence, the model is intended for optimized high-quality percussion drilling without excessive influence of melt. For this case, the considered situation is sketched in Fig. 1. In Fig. 1 a), the laser beam incident on the workpiece is assumed to have a Gaussian fluence profile (blue curve) with a beam radius  $w_0$ .

The entrance radius  $r_{abl}$  of the laser-drilled hole is then given when the Gaussian function is evaluated for the threshold fluence,

$$\phi_{th} = \phi_0 \cdot \exp\left(-\frac{2 \cdot r^2}{w_0^2}\right) \quad (1)$$

Here  $\Phi_0$  denotes the peak fluence which is given by

$$\phi_0 = \frac{2 \cdot E_p}{\pi \cdot w_0^2} \quad (2)$$

where  $E_p$  is the pulse energy. Then the entrance radius of the hole  $r_{abl}$  amounts to

$$r_{abl} = w_0 \cdot \sqrt{\frac{1}{2} \ln\left(\frac{\phi_0}{\phi_{th}}\right)} \quad (3)$$

As no ablation can take place on the surface of the workpiece beyond the radius  $r_{abl}$ , this corresponds to the size of the opening of the drilled hole. As mentioned above the growth of the hole into the depth produced by percussion drilling will eventually stop and typically have a conical geometry with a depth  $z_{drill}$  as shown in Fig. 1 b). Due to multiple reflections, the fluence is homogeneously distributed within the hole. In contrast to results from raytracing or similar methods, which show a concentration of energy at the bottom of a hole with ideal flat surfaces, an increasing roughness of the walls of the drilled hole and scattering on particles are assumed to lead to a diffuse distribution of the radiation within the bore hole. Even for ideal flat surfaces a homogenization of the radiation within a bore hole takes place [14]. If inhomogeneities along the walls of a drilled hole are introduced, wave optics calculations show significant disturbance of the absorbed intensity distribution [8]. The model for the diffuse scattering of radiation within a cavity goes back to 1945 [15,16] and has been successfully used to model the absorption of laser radiation in vapor capillaries during laser welding [17–19]. In the following, the model using diffuse scattering is applied to the laser drilling process.

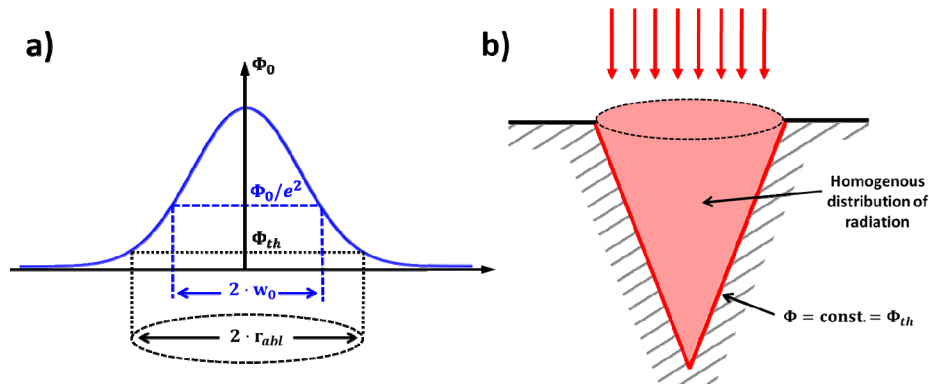


Fig. 1. a) Incident lateral fluence profile (idealized Gaussian, blue). b) Conical geometry at the time of termination of the drilling process with homogenous fluence distribution (red)

When the incident energy  $E_p$  is homogeneously distributed in the conically shaped final hole which is shown in Fig. 1b), the resulting fluence yields

$$\phi_{th} = \frac{E_p}{\pi \cdot r_{abl} \cdot \sqrt{r_{abl}^2 + z_{drill}^2}} \quad (4)$$

where the denominator is equal to the area of the walls of the drilled hole. As  $r_{abl}$  and  $z_{drill}$  characterize the geometry of the final hole, when the drilling progress comes to a stop as described above, the fluence expressed in Eq. (4) corresponds to the ablation threshold for a large number of pulses ( $> 10^3$ ), where the threshold as a function of the number of pulses stays constant [20].

Inserting Eq. (2) into Eq. (4) and solving for  $z_{drill}$  this can be converted to the ratio

$$\frac{z_{drill}}{w_0} = \sqrt{\frac{\phi_0^2 - \phi_{th}^2 \cdot \ln^2\left(\frac{\phi_0}{\phi_{th}}\right)}{2 \cdot \phi_{th}^2 \cdot \ln\left(\frac{\phi_0}{\phi_{th}}\right)}} \quad (5)$$

which is a generalized expression for the hole depth  $z_{drill}$  achievable with a given beam radius  $w_0$  and the ablation threshold of a given material. It only depends on the ablation threshold  $\Phi_{th}$  and the peak fluence  $\Phi_0$  of the incident Gaussian distribution and therefore allows comparing different percussion drilling processes directly as long as the materials to compare have the same ablation threshold. In the following section, this expression is evaluated for stainless steel and different focusing conditions.

### 3. Experimental verification

Percussion drilling experiments were performed to verify the prediction expressed by Eq. (5). To exclude a deterioration of the quality by heat accumulation and excessive melt, an ultrafast solid-state laser (Duetto, Lumentum) was used at a repetition rate of 5 kHz. The wavelength of the laser is 1064 nm and the maximum pulse energy amounted to 160  $\mu$ J. The pulse duration was 10 ps and the laser beam was circularly polarized. Three different focal lengths (340 mm, 170 mm, and 77 mm) were used to focus the Gaussian laser beam (see spatial beam profile in Fig. 2) to three different focal radii of 45  $\mu$ m, 23  $\mu$ m, and 13  $\mu$ m which correspond to the maximum peak fluences  $\Phi_0$  of 5.0 J/cm<sup>2</sup>, 19.3 J/cm<sup>2</sup> and 60.3 J/cm<sup>2</sup>. The focal plane was on the surface of the drilled sample.

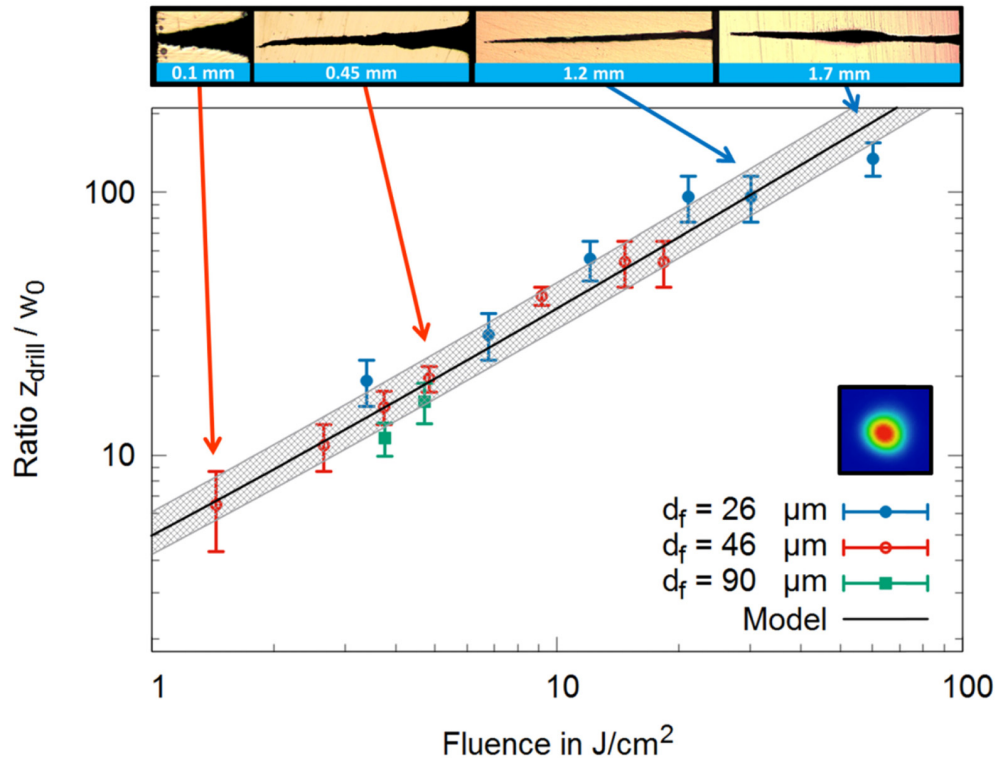


Fig. 2. Experimental results (data points with error bars) and the ratio  $z_{drill}/w_0$  calculated from the simplified model (black line with surrounding hatch, standing for a model with an ablation threshold of  $0.09 \pm 0.02 \text{ J/cm}^2$ ). Exemplary cross sections of one through hole and several blind holes are shown at the top. After recording the pictures, the contrast was artificially increased by image processing software. The spatial beam profile of the used ps laser is given in the inset on the right.

The focal diameters were measured by means of beam profiling cameras (WinCamD, Dataray Inc. or FM100, Metrolux GmbH). The achievable hole depth was investigated by drilling through steel plates of different thicknesses ranging from 0.1 mm to 1 mm in steps of 0.05 mm. At high fluence additional experiments were performed on samples with a thickness of 1.5 and 2 mm.

After drilling, the holes were first examined by the eye and second by a microscope with underside illumination to determine the maximum plate thickness that was drilled through as well as the minimum plate thickness that was not drilled through for a given focal diameter and pulse energy (i.e. fluence). To find a set of parameters leading to a hole that was drilled through, the examinations by eye and microscope were sufficient.

To clarify for how long the experimental drilling process has to be continued to be able to decide that a hole cannot be drilled through with the given parameters, the following consideration was used. If a single pulse contributes to the drilling process, it must be able to ablate at least one single atomic layer, which has a thickness of  $3 \text{ \AA}$ . One atomic layer is the minimum depth that can be ablated by a single pulse (otherwise the atoms would have to be fissioned). If in the worst case every pulse only ablates one atomic layer, the number of pulses needed to drill through a defined thickness is given by the thickness divided by  $3 \text{ \AA}$ . In our experiments we therefore always applied this amount of pulses to be sure that a given sample thickness cannot be drilled through. For a plate with a thickness of  $600 \text{ \mu m}$ , for example, 2 million pulses needed to be applied. At a repetition rate of 5 kHz this amounts to a drilling time of 400 seconds. If a  $600 \text{ \mu m}$  thick plate was not drilled through after this time, it was

defined as not being drilled through. For the 2 mm thick samples, the maximum required drilling time amounted to 22 minutes and 13 seconds.

The average between the maximum plate thickness that was drilled through and the minimum plate thickness that was not drilled through was used as the experimentally determined value of  $z_{drill}$ , and the difference of the two values was used as the measure of the uncertainty. Figure 2 shows the ratio  $z_{drill}/w_0$  of the percussion-drilled holes as a function of the peak fluence of the beam incident on the workpiece surface. The data points with the error bars for the mentioned uncertainty are the experimental results for the three different focal lengths  $f = 340$  mm,  $f = 170$  mm, and  $f = 77$  mm. The black line is given by Eq. (5) assuming an ablation threshold of  $0.09$  J/cm<sup>2</sup>. The gray shaded area is given by Eq. (5) assuming a variation of the ablation threshold of  $\pm 0.02$  J/cm<sup>2</sup>. The chosen threshold fluence coincides well with values given by other authors, ranging from  $0.05$  J/cm<sup>2</sup> to  $0.15$  J/cm<sup>2</sup> [10,22,23] for the same type of steel (St 1.4301 or AISI 304) and for the same pulse durations and wavelength. The good agreement between the experimental results and the theoretical model shows the usefulness of the simple model. The model can be used to estimate the maximum achievable depths of percussion-drilled holes only based on the ablation threshold of the material and the radius of the incident laser beam. Cross sections of some exemplary blind holes are additionally shown on the top of Fig. 2. The conical shape obviously dominates the final geometry of the drilled holes. If there are deviations from this geometry, e.g. for  $60$  J/cm<sup>2</sup> (right picture), the model is not fully suitable to describe the maximum achievable drilling depth. Instead, for this case the achievable hole depth is slightly lower than the one predicted by the model. This is mainly due to a particle-ignited plasma, which can occur at high fluences for pulse durations of several picoseconds [24,25]. The final area within such a hole then is larger than the one of a pure conical hole due to the formed bulge in the middle of the hole. Still, in principal the introduced model allows to perform an estimation of the achievable hole depths and aspect ratios when the laser machining tool is well characterized and the ablation threshold of the material is known. The model should be valid for a large variety of isotropic and non-transparent materials.

#### 4. Percussion drilling of deep holes

As a further example, the proposed model was applied to determine the requirements for percussion drilling of unconventionally deep holes. Generally speaking, the drilling of deep holes is motivated by the necessity to transport fluids. Possible applications are the nebulization of coolants [4] or combustion materials [3], the production of cellulose fibers [26], and the delivery of lubricants [4]. For lubricant supply, a hole in 10 mm thick steel and with an outlet diameter of several  $10$   $\mu$ m needed to be produced. Reasonable focal diameters in laser precision manufacturing lie in the range of  $20$   $\mu$ m to  $250$   $\mu$ m. Equation (5) states that for a focal diameter of  $20$   $\mu$ m, a pulse energy of approximately  $600$   $\mu$ J is needed, while for  $250$   $\mu$ m it amounts to approximately  $6$  mJ. In order to cover this range of pulse energies, a previously developed multi-pass thin-disk laser amplifier [21] emitting an average power of  $1.1$  kW was used. It was already shown before that when drilling deep holes with high fluences the repetition rate should be close to  $30$  kHz or lower in order to avoid heat accumulation effects [5]. The repetition rate of the laser system was therefore reduced to  $30$  kHz, which resulted in a maximum pulse energy of  $3$  mJ and hence in an average power of  $90$  W. According to Eq. (5), the use of focal radii of  $59$   $\mu$ m or smaller at this maximum pulse energy of  $3$  mJ then results in a hole with a depth of  $10$  mm. Since the used laser beam profile was of elliptical shape (cf. Figure 3), it was finally focused with a lens with a focal length of  $160$  mm in order to achieve a beam radius of  $w_{0,x} = 53$   $\mu$ m ( $1/e^2$  major semi-axis) by  $w_{0,y} = 38$   $\mu$ m ( $1/e^2$  minor semi-axis). The corresponding Rayleigh ranges therefore amounted to  $z_{R,x} = 6.6$  mm and  $z_{R,y} = 3.4$  mm.

Mirrors guided the beam through the experimental setup, passing a quarter-wave plate to obtain a circularly polarized beam. The chosen focusing lens with a focal length of 160 mm focused the beam finally onto the surface of the workpiece of 10 mm thickness.

A cross-section of the resulting hole after the percussion drilling process is shown in Fig. 3. After the cutting and polishing of the sample, it was etched in Adler etchant (solution of water, ammonium chlorocuprate, hydrochloric acid and ferric chloride). As can be seen, no thermal damage (structural change) occurred, which is due to the low repetition rate used for drilling. The drilled holes exhibit the typical predominantly conical geometry. The ratio  $z_{drill}/w_0$  of the produced hole amounts to approximately 189 or 263, depending on the semi-axis of the beam profile that is used as a reference. The aspect ratio of the hole, hence the depth divided by either the entrance or the outlet diameter, amounts to 24.4 or 192, respectively.

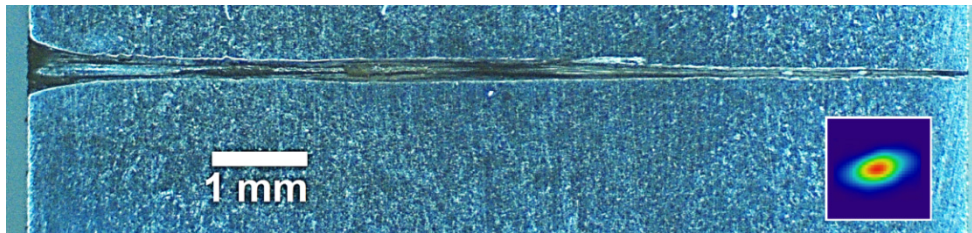


Fig. 3. Through hole in 10 mm stainless steel (St 1.4301 / AISI 304), etched (Adler etchant); entrance diameter approx. 410  $\mu\text{m}$  (left side), outlet diameter approx. 52  $\mu\text{m}$  (right side); the beam profile of the used high-energy ps laser is displayed in the inset on the right. After recording the picture, the contrast was artificially increased by image processing software. The number of pulses required to create this hole amounted to 12.2 million, resulting in a drilling time of 6 minutes and 48 seconds and an average drilling rate of 8.2  $\text{\AA}$  per pulse.

## 5. Conclusion

In summary, we have shown that a simplified model based on the assumption of a conical borehole geometry can be used to predict the achievable drilling depth or aspect ratio of percussion drilling processes. A homogeneous intensity distribution was assumed when the drilling process stops. Based on this assumption, a basic equation for the achievable depth was derived which only depend on the applied fluence, the beam radius, and the ablation threshold of the material. It is suggested by the authors that the introduced model depending on the homogeneous distribution of energy describes a quality limit of laser drilling, as for example described as “phase 1” in [8]. If effects such as nonlinear absorption and heat accumulation are avoided, the model correctly describes the achievable drilling depths.

The validity of the model was confirmed by corresponding drilling experiments. In this context it was shown that it is possible to design a drilling process to achieve a hole with a depth of 10 mm.

## Funding

DFG (grant number GR 3172/21-1); Baden-Württemberg Stiftung (grant number MAT0054).

## Acknowledgment

The authors thank L. Hoster for polishing and etching the samples.